

5796  
NACA TN 3357

TECH LIBRARY KAFB, NM  
01.52230

# NATIONAL ADVISORY COMMITTEE FOR AERONAUTICS

TECHNICAL NOTE 3357

THE EFFECTS OF VARIOUS PARAMETERS, INCLUDING MACH  
NUMBER, ON PROPELLER-BLADE FLUTTER WITH  
EMPHASIS ON STALL FLUTTER

By John E. Baker

Langley Aeronautical Laboratory  
Langley Field, Va.



Washington  
January 1955

AFM C  
TECHNICAL NOTE  
AFL 2011



## NATIONAL ADVISORY COMMITTEE FOR AERONAUTICS

## TECHNICAL NOTE 3357

THE EFFECTS OF VARIOUS PARAMETERS, INCLUDING MACH  
NUMBER, ON PROPELLER-BLADE FLUTTER WITH  
EMPHASIS ON STALL FLUTTER<sup>1</sup>

By John E. Baker

## SUMMARY

The effects of many of the parameters significant to wing flutter were studied experimentally on several untwisted rotating models to determine their significance with respect to stall flutter of propeller blades. The parameters included torsional stiffness, section thickness ratio, sweepback, length-chord ratio, section center-of-gravity location, blade taper, Mach number, and fluid density. In order to check on the effects of blade twist, one model which had spanwise twist was studied. The blade angles of the models were generally varied from low values to beyond the stall.

The experimental results for the flutter speed are presented in the form of flutter-speed coefficients  $(V/b\omega_\alpha)_{0.8L}$ , where the quantities  $V$  and  $b$  are the resultant velocity and semichord, respectively, taken at 0.8 blade length  $L$ , and  $\omega_\alpha$  is the natural first-torsion circular frequency of the blade. The minimum values of this flutter-speed coefficient were found to be slightly greater than 1.0 for subcritical Mach numbers. The parameters that produced a significant increase of this flutter-speed coefficient were forward movement of the section center-of-gravity location, sweepback, increase of the section thickness ratio, and Mach number at supercritical speeds. In order to maintain satisfactory aerodynamic efficiency at high speeds, however, thin blade sections are required. The largest effects on the flutter-speed coefficient were produced by the section center-of-gravity location and the Mach number. The effect of Mach number was of such significance that it is possible to present a tentative criterion for designing completely flutter-free thin propeller blades to operate at supersonic and supercritical speeds. This criterion is given by the design parameter  $(b\omega_\alpha/c)_{0.8L}$  (where the quantity  $c$  is the sound speed of the operating medium) and the present investigation indicates that propeller blades having values of this parameter above 0.50 should be entirely free of flutter. It is also

<sup>1</sup>Supersedes the recently declassified NACA RM L50L12b, "The Effects of Various Parameters Including Mach Number on Propeller-Blade Flutter With Emphasis on Stall Flutter" by John E. Baker, 1950.

possible to consider various operating procedures for propellers not satisfying the criterion as a means for avoiding flutter.

## INTRODUCTION

The propeller-flutter problem is an old one. Papers have been written on the subject from World War I to the present, and some of the significant results are summarized in reference 1. In the past, propeller flutter has been studied primarily by trial-and-error methods on specific propellers. Therefore, much confusion and contradictory data exist at the present time.

In general, flutter can be avoided by making the blade sections sufficiently thick; however, recent aerodynamic investigations have shown that propellers for future high-speed aircraft must be thin in order to obtain satisfactory performance. Thus, propeller flutter, which has been considered chiefly as a nuisance in the past, now becomes a critical design problem. The trial-and-error methods of the past have become inadequate for the design of thin supersonic and transonic propellers. Accordingly, a fairly comprehensive experimental study has been made to determine the effects of various parameters on propeller flutter. The parameters studied include torsional stiffness, section thickness ratio, sweepback, length-chord ratio, section center-of-gravity location, blade taper, blade twist, Mach number, and density of the operating medium. Blade angles were generally varied from low lift to beyond the stall.

Propeller flutter, as described, for example, in references 2 and 3, can be separated into two main types, classical flutter and stall flutter. Classical flutter exists at low angles of attack where the flow can be considered potential and, hence, the aerodynamic forces can be evaluated by the use of potential-flow theory. Stall flutter is encountered at high angles of attack where the flow is broken down and potential theory fails to apply. Classical flutter is generally characterized by a coupling of the bending and torsion vibration modes; whereas stall flutter occurs primarily in the torsion mode. The classical-flutter frequency usually falls between the first-torsion and first-bending frequencies, but the stall-flutter frequency is nearly the same as the natural first-torsion frequency of the blade. There is no definite boundary between stall flutter and classical flutter, and a continuous merging exists. The natural phenomena involved in this merging are still uncertain although various attempts have been made to associate them with the behavior of the static lift curve. Stall-flutter speeds have been found to be lower than classical-flutter speeds.

The designer is primarily interested in being able to calculate the propeller-flutter conditions in connection with the possible operating

conditions. At the present time, no theories are established that can predict adequately stall-flutter speeds, but some theories exist that apply to classical flutter of propellers, (references 4 to 6) and a brief discussion of these theories is given.

Propellers under normal flight conditions generally operate with the blade sections at low angles of attack and would be subject to classical flutter. Under these operating conditions, the flutter speed is high, and generally there is an appreciable margin of safety between the operating speed and the flutter speed; however, during the take-off period, the propeller blade sections may operate at high angles of attack and would be subject to stall flutter. Under these operating conditions, the flutter speed is generally quite low, and the propellers must operate near the flutter condition where the margin of safety is fairly small. As a consequence, propellers are required to operate in the stalled condition without dangerous flutter. Since stall flutter is the critical design condition, and because no adequate theories are established for predicting stall-flutter speeds for propellers, the investigation was devoted primarily to obtaining information on stall flutter, and, in particular, the minimum stall-flutter condition.

#### SYMBOLS

$A_{ch}$	}	potential nonsteady aerodynamic coefficients
$A_{c\alpha}$		
$A_{sh}$		
$A_{s\alpha}$		
$a$	nondimensional elastic axis position referred to semichord measured from midchord	
$b$	blade semichord, feet	
$b_r$	blade semichord at reference station, feet	
$c$	sound speed of operating medium, feet per second	
$c_l$	section lift coefficient	
CG	section center-of-gravity location, percent chord	
$G$	shear modulus of elasticity, pounds per foot <sup>2</sup>	
GJ	torsional stiffness, pound-feet <sup>2</sup>	
EA	elastic axis location, percent chord	

$f_{\alpha}$	blade first-torsion frequency, cycles per second
$f_h$	blade first-bending frequency, cycles per second
$F_h(\eta)$	blade-bending-deflection function in terms of tip deflection
$F_{\theta}(\eta)$	blade-torsional-deflection function in terms of tip deflection
$\xi_h$	structural damping coefficient in bending as used in reference 7
$\xi_{\alpha}$	structural damping coefficient in torsion as used in reference 7
$\underline{h}$	bending deflection of blade, feet
H	hub radius, feet
$I_{\alpha}$	polar moment of inertia about elastic axis per unit length, slug-feet <sup>2</sup> per foot
$I_{CG}$	polar moment of inertia about the section center-of-gravity location per unit length, slug-feet <sup>2</sup> per foot
k	reduced frequency ( $b\omega/V$ )
L	blade length, feet
M	Mach number
m	blade mass per unit length, slugs per foot
$r_{\alpha}^2$	nondimensional radius of gyration of blade section about elastic axis ( $I_{\alpha}/mb^2$ )
$r_{CG}^2$	nondimensional radius of gyration of blade section about the section center-of-gravity location ( $I_{CG}/mb^2$ )
t	section thickness, feet
V	resultant velocity, feet per second
X	distance from blade root, feet
$x_{\alpha}$	nondimensional center-of-gravity position measured from elastic axis in terms of semichord
$\beta$	blade angle, degrees

$\mu$	mass density of blade material, slugs per cubic foot
$\eta$	nondimensional distance from blade root ( $X/L$ )
$\eta'$	nondimensional distance from center of rotation $\left(\frac{X+H}{H+L}\right)$
$\theta$	torsional deflection of blade, radians
$\kappa$	blade mass-density ratio ( $\pi\rho b^2/m$ )
$\rho$	mass density of operating medium, slugs per cubic foot
$\sigma$	blade solidity at $0.8L$ ( $2b/2\pi(0.8L+H)$ )
$\phi$	aerodynamic helix angle, degrees
$\omega$	blade circular flutter frequency, radians per second
$\omega_h$	blade circular first-bending frequency ( $2\pi f_h$ ), radians per second
$\omega_\alpha$	blade circular first-torsion frequency ( $2\pi f_\alpha$ ), radians per second

#### APPARATUS AND TEST METHODS

The apparatus and testing techniques herein described are similar to those used in the tests of reference 2. The propeller models were operated in the Langley vacuum sphere in which provisions are made for operating in air or Freon-12. Freon-12 is a convenient medium for studying the effects of Mach number because its sound speed is about 500 feet per second at room temperature (reference 8). The propeller models were rotated by means of a 500-horsepower electric motor (fig. 1) and operated at zero forward velocity except for induced flow. Bending and torsion oscillations of the blade were recorded by an oscillograph with the aid of wire strain gages on the blade (see sample record in fig. 2). The rotational speed was also recorded on the same record, which, for zero forward velocity, is equivalent to the resultant velocity. A few total-pressure measurements were obtained in the wake by means of a survey rake located about 0.17 propeller diameter behind the propeller disk.

Flutter runs were generally made in air at  $1/4$ ,  $1/2$ , and  $1.0$  atmosphere pressure, but only the data obtained at  $1.0$  atmosphere are presented herein, with the exception of data for the studies of density

and Mach number. Blade angles were usually varied from low lift to beyond the stalling angle. Flutter was not studied at zero thrust on the untwisted blades because wake flutter, such as that described in reference 3, occurred. During each flutter run, the rotational speed was gradually increased until flutter was observed, at which point a record was taken. A few attempts were made to go through the flutter region at stall, but the flutter was usually too violent to do so.

The effect of Mach number was studied by operating in various mixtures of air and Freon-12 in order to vary the sound speed of the operating medium. This technique made it possible to obtain a range of Mach numbers at any given rotational speed. The density was held constant at about 0.0011 slug/cubic foot for the various mixtures by varying the pressure of the operating medium.

The flutter models with their identifying numerical designations and their significant parameters are listed in table I. The parameters studied, the range of values covered, and the models used to study them are described in table II. Information about the blades, which is not listed in tables I and II, is described as follows:

(1) The sweptback models were swept from a radial line with the sweepback beginning at the root of the blade, as indicated by the dashed outline in figure 1.

(2) Models 1a and 1b were successively shortened to change the length-chord ratio.

(3) The section center-of-gravity location was varied by the use of different blades with brass inserts cycle-welded in the blades near the leading edge so that the section contour remained unaffected.

(4) Model 2 was nearly identical to model 1a and was twisted manually to beyond the yield stress, resulting in a set twist of  $17^\circ$  at the tip, and the angle of twist varied linearly along the span.

## RESULTS AND DISCUSSION

### Considerations on Method of Presentation

Reference section.- The experimental data are presented showing the effects of the various parameters studied on the flutter-speed coefficients. The data shown are all referred to the 0.8-blade-length position which, for propellers having large hub diameters, would result in a more representative reference section than would result if a standard radius location were used.

Lift coefficient.- The blade angles shown are the blade-angle settings at 0.8 blade length referred to the plane of rotation. The relation between blade-angle setting and lift coefficient is distorted because of the effects of induced flow and blade twisting due to centrifugal forces and aerodynamic forces. Since the designer is primarily concerned with lift coefficient, some of the wake-survey data were evaluated to yield lift coefficients. The individual wake surveys are incomplete and, as a consequence, considerable scatter of the pressure measurements is present; however, as a matter of interest, a band showing the approximate values of experimental lift coefficients corresponding to the various blade-angle settings is shown in figure 3. This figure is applicable in general to the models having 0.333-foot chord and blade length of 1.788 feet, with which most of the low Mach number data were obtained.

Flutter-speed coefficient.- The flutter velocity is a function of a great number of parameters:

$$\frac{V}{b\omega_{\alpha}} = f\left(\frac{\omega_n}{\omega_{\alpha}}, \kappa, a, x_{\alpha}, r_{\alpha}^2, \frac{L}{b}, M, c_l, \dots\right)$$

The ratio  $V/b\omega_{\alpha}$  is designated as the flutter-speed coefficient, the value of which is dependent on the large number of parameters. This coefficient is taken at a reference section which is 0.8L for the data shown herein. The purpose of this investigation is to determine the effects of many of these parameters on the flutter-speed coefficient. Before discussing the effect of the parameters studied on this coefficient, it appears advisable to point out the significance of the flutter-speed coefficient and its component parts in order to interpret correctly the applicability of the data presented herein. For comparison purposes, assume that a certain flutter-speed coefficient is given, in other words,

$$\frac{V}{b\omega_{\alpha}} = \text{Constant}$$

For this condition, an increase in the semichord is accompanied by a proportional increase in the flutter speed provided the torsional frequency remains constant.

The semichord can be varied without changing the torsional frequency if the airfoil section is unchanged, as is illustrated by considering the first-torsion frequency equation for a uniform beam:

$$\omega_{\alpha} = \frac{\pi}{2L} \sqrt{\frac{GJ}{I_{\alpha}}}$$

$$J \approx A(2b)t^3 \quad \text{where } A \text{ is a constant}$$

$$I_{\alpha} \approx Bt(2b)^3 \quad \text{where } B \text{ is a constant}$$

Then

$$\omega_{\alpha} \approx \frac{\pi}{2L} \sqrt{\frac{GA(2b)t^3}{B_{\mu}t(2b)^3}} = \frac{t}{2b} \frac{\pi}{2L} \sqrt{\frac{GA}{B_{\mu}}} \quad (1)$$

For a given value of the flutter-speed coefficient, increasing the torsion frequency will be accompanied by a proportional rise in the flutter velocity if the chord at the reference section is held constant. It can be seen in equation (1) that two methods of raising the torsional frequency are increasing the section thickness ratio and decreasing the blade length. Reference 9 indicates that tapering the blade chord will also raise the torsional frequency.

Appropriate care should thus be exercised in the interpretation, in terms of actual flutter speeds, of results which are presented as flutter-speed coefficients.

#### Experimental Data and Discussion

The parameters studied and the figures in which the data are presented are listed in table II. In the experimental investigation, the various parameters were isolated where possible, and, correspondingly, the data showing the effects of each parameter are presented in separate figures. In figures 4 to 11, the ordinate is the flutter-speed coefficient  $(V/b\omega_{\alpha})_{0.8L}$  and the abscissa is blade angle  $\beta_{0.8L}$ . The parameters studied are torsional stiffness (fig. 4), blade taper (fig. 5), blade twist (fig. 6), length-chord ratio (fig. 7), density of the operating medium (fig. 8), section thickness ratio (fig. 9), sweepback (fig. 10), and section center-of-gravity location (fig. 11). The effects of Mach number are shown in figure 12, where flutter-speed coefficients for a given blade angle are plotted as a function of Mach number. These parameters are discussed in this section. It is noted that many of the flutter curves are not completely filled in at low blade angles. For these cases, the flutter speed has become higher than the maximum safe operating speed of the blades.

The flutter data given in figures 4 to 11 were obtained under conditions of subcritical flow, that is, with subcritical operating speeds at the reference section. A significant observation can be made from a study of the minimum values of the flutter-speed coefficients that occur for each parameter studied; namely, the lowest value obtained for each parameter is slightly greater than 1.0. Deviations from this value are, therefore, used as a basis of comparison for variations of each parameter.

Parameters having little effect on the minimum flutter-speed coefficients.— The parameters that produced no significant increase of the

minimum flutter-speed coefficients are torsional stiffness, blade taper, blade twist, length-chord ratio, and density of the operating medium (figs. 4 to 8). As has been pointed out, the minimum flutter-speed coefficients may be unaffected by changing a given parameter, but the product  $b\omega_{cr}$  should be examined to determine the effect of the changes on the flutter speed.

In contrast to the insignificant effect of torsional stiffness on the minimum flutter-speed coefficient, a large effect on the flutter-speed coefficient at low blade angles is indicated by the data in figure 4. This effect is in accord with the theory for classical flutter.

Section thickness ratio.- Increasing the section thickness ratio is shown to have some effect on the minimum flutter-speed coefficients by the data in figure 9. Increase of the section thickness ratio from 6 to 9 percent chord raised the minimum flutter-speed coefficient about 20 percent; however, thick blade sections are associated with greater reductions in aerodynamic efficiency at transonic speeds.

Sweepback.- The flutter data in figure 10 indicate that moderate amounts of sweepback raised the minimum flutter-speed coefficient about 30 percent. In view of the serious structural problems associated with sweptback propeller blades, this moderate rise in minimum flutter-speed coefficient does not appear to be of much practical significance.

Section center-of-gravity location.- A pronounced effect of section center-of-gravity location is indicated by the flutter data in figure 11. Forward movement of the section center-of-gravity from 48.5 to 37.4 percent chord resulted in a rise of the minimum flutter-speed coefficient of about 60 percent. At 34.0 percent chord, the minimum flutter-speed coefficient was about 80 percent higher than that for the section center-of-gravity at 48.5 percent chord.

This favorable effect of forward movement of the section center-of-gravity location cannot be utilized to a great extent for solid blades but, for built-up or hollow sections, some forward movement of the section center-of-gravity location can be realized. However, forward movement of the section center-of-gravity location for operation at supersonic speeds may result in some unfavorable conditions. For example, centrifugal force causes the effective elastic axis of propeller blades to approach the section center-of-gravity location. The aerodynamic center of pressure is shifted from the subcritical value of quarter chord to about midchord at supersonic speeds. If the section center of gravity is located far forward, the aerodynamic pitching moment about the section center-of-gravity location at supersonic speeds would become negative. This negative pitching moment would then add to, rather than oppose, the negative pitching moment due to centrifugal force, probably resulting in excessive torsional deflections.

The data in figure 11 indicate that forward movement of the section center-of-gravity location has an extremely great effect on the flutter-speed coefficients at low blade angles. This effect is to be expected from classical-flutter theory.

Mach number.- The effect of Mach number on the minimum flutter-speed coefficients is beneficial, as is indicated by the data in figure 12 for two blades each at a constant blade angle. The blade angles were chosen to be the angles at which the minimum flutter-speed coefficients were obtained on each blade, as shown in figure 5. In figure 12, the coefficients remain nearly constant at about 1.1 to 1.2 up to the vicinity of the critical Mach number at the reference section. Further increases of Mach number result in a rapid rise of the flutter-speed coefficients.

It is to be noted in figure 12(b) that flutter was encountered at several points in the supposedly stable region at a  $(V/b\alpha_x)_{0.8L}$  of 1.7 at a rotational frequency of one-eighth the blade torsional frequency. The oscillation encountered is very likely caused by strut interference since there are four struts supporting the motor. Further indication of interference is supplied by the fact that the range of speeds at which these oscillations were observed is very narrow.

The significance of the influence of Mach number is better illustrated by replotting the experimental flutter curve in figure 12(b) in the form shown in figure 13. If, in the flutter-speed coefficient, both the numerator and denominator are divided by the speed of sound, the two nondimensional coefficients, Mach number and  $b\alpha_x/c$  are obtained, both taken at 0.8 blade length. These quantities are used as ordinate and abscissa in figure 13. Straight lines radiating from the origin indicate constant flutter-speed coefficients. The value of  $(b\alpha_x/c)_{0.8L}$  at which the turning point of the flutter curve occurs is considered to be of fairly general significance. This conclusion is confirmed by test points obtained from whirl tests of full-scale propellers made at Wright-Patterson Air Force Base and by different manufacturers. Since the experimental flutter curve in figure 13 is for the blade angle at which the minimum flutter-speed coefficient occurred, data at either lower or higher blade angles should fall above and to the left of the given instability curve. The portion of the instability curve above the turning point could not be investigated with the apparatus available for these studies since the flutter encountered was too severe. A given propeller would operate on a vertical line designated by a constant value of  $(b\alpha_x/c)_{0.8L}$  for a fixed speed of sound. It can be seen that, for blades having low values of  $(b\alpha_x/c)_{0.8L}$  and operating at the stall condition, this line would intersect the flutter curve before supersonic speeds are reached, and the blades would experience flutter. However, it may be possible to design satisfactory thin propeller blades

with  $(b\omega_\alpha/c)_{0.8L}$  great enough to permit operation into the supersonic speed range without intersecting the flutter boundary.

#### Possible Applications

A design criterion.- A tentative design criterion based on these data can be determined and indicates that propellers having values of the design parameter  $(b\omega_\alpha/c)_{0.8L}$  greater than 0.50 should be entirely free of flutter. Many current propellers giving satisfactory service at tip Mach numbers near 1.0 have values of the design parameter near 0.40. These propellers may flutter at the stall, but whirl tests established any flutter which may have been encountered as nondestructive. The value of 0.50 is used for the criterion presented because thin blades probably could not endure flutter without the danger of fatigue.

Some blade configurations based on the given design criterion are shown in figure 14. Two designs of constant thickness ratio are shown, although structurally this condition may not be too practical. Another blade having taper in thickness ratio and constant chord, which may be more acceptable, is also shown. These blade configurations may not be ideal in some respects, but it appears possible to construct supersonic-type propellers with  $(b\omega_\alpha/c)_{0.8L}$  greater than 0.50 and, consequently, to be completely free of flutter.

A cycling process.- Many of the supersonic-type experimental propellers being considered at the present time have values of  $(b\omega_\alpha/c)_{0.8L}$  of the order of 0.10 to 0.20. It can be seen in figure 13 that such propellers would flutter if attempts were made to accelerate them to supersonic speeds at the stall condition. There is a possibility that these propellers can still be operated at supersonic speeds at stall without flutter if they are brought up to speed in a manner to be described.

The flutter-speed coefficient at some blade angle lower than the stalling blade angle would be greater and would appear in figure 13 as a line from the origin of greater slope. The lower lift coefficient would raise the critical Mach number, and thus the flutter curve at some unstalled blade angle should be similar to the dashed curve in figure 13. The experimental flutter curve is extended in the direction it might be expected to go by the dotted line. A propeller having  $(b\omega_\alpha/c)_{0.8L}$  of say 0.4 would intersect with the flutter curve if attempts were made to bring it up to supersonic speeds at  $20^\circ$  blade angle; however, it could be accelerated to supersonic speeds at the lower blade angle without fluttering. Once the propeller is up to speed, the blade angle could be increased to  $20^\circ$  without experiencing flutter since this condition would be above the upper limit of the flutter boundary. It is necessary, however, that the operating speed is not reduced enough to intersect with the flutter curve due to the increased power loading. The reverse of this operating cycle would have to be followed in stopping the propeller if flutter is to be avoided.

This so-called cycling process necessitates close attention to other parameters which are critical to the low angle-of-attack classical-flutter speeds, and involves primarily torsional stiffness. The data in figure 4 demonstrate the great effect of torsional stiffness on the flutter speed at low blade angles. A critical condition for successful cycling is that the classical-flutter speed is appreciably higher than the maximum operating speed. This condition exists when  $(b\omega/c) > 0.8L$  for a given propeller does not intersect the flutter curve for the blade angles at which the propeller is brought up to speed.

Operation above the flutter boundary.- The flutter at the minimum of the low-speed flutter curves was generally much less violent than the flutter at lower blade angles. Attempts were made to operate some of the test models into the flutter region. At blade angles corresponding to the minimum of the flutter curve, some of the blades were operated successfully without dangerous flutter at higher speeds than those indicated by the flutter curve; however, the density of the operating medium usually had to be reduced considerably before successful operation resulted. At lower blade angles, the flutter region could not be penetrated without the flutter becoming very severe.

#### Comparison of Experiment with Classical-Flutter Theory

As previously discussed, propeller flutter can be separated into two main types, classical flutter which occurs at low angles of attack and stall flutter which is associated with high angles of attack and which occurs at lower speeds than does classical flutter. Since the designer is interested in being able to predict flutter speeds, a survey of existing theoretical techniques is desirable.

At present, no theories are established that can adequately predict stall-flutter speeds for propellers. However, in order to make effective use of cycling procedures, knowledge of classical-flutter speeds is desirable, so some of the available classical propeller-flutter theories (references 4 to 6) will be discussed briefly. The theory of reference 4 uses a differential-equation approach similar to that used in wing-flutter theory, but, in addition, introduces centrifugal force and moment into the equations. Reference 5 uses the same attack to the problem, but with more simplifying assumptions which eases numerical application somewhat. The theory of reference 6 utilizes known wing-flutter theory in a manner similar to references 4 and 5. The effect of centrifugal force is included in the bending mode, but neglected in the torsion mode. Classical two-dimensional oscillating air forces are used in all three theories, and reference 6 has provisions for using either compressible or incompressible values. Some computations have been made in order to compare theoretical with experimental results presented herein. The theories referred to are quite difficult to adapt to numerical calculations and generally require considerable computing time. The theory of reference 5, however, with certain modifications, was used to compute one case.

The theory of reference 5 was developed for application to helicopter rotors with the assumption that the root of the blade is located at the center of rotation. This assumption does not lead to great errors when applied to helicopters because the hub diameter is generally small with respect to the rotor diameter. Since propellers have much larger hubs, the theory of reference 5 had to be modified to make use of a hub radius, which may be as much as 30 percent of the propeller radius. The modified theory was used to compute the classical-flutter speed of model 4, and the result is shown in column (1) of table III.

Since the existing propeller-flutter theories are quite cumbersome, a classical wing-flutter theory (reference 10) was modified to apply to propellers. This modification was accomplished by allowing the aerodynamic forces to vary along the blade and applying centrifugal-force corrections to the static first-bending and first-torsion frequencies. This method of analysis is discussed in the appendix. The dynamic deflection curves were assumed to be the same as for the static case. This method was used to compute classical-flutter speeds for three of the models used in the current tests, and the results are shown in table III column (2).

A comparison of theoretical values in column (2) of table III with experimental results in columns (5) and (6) of table III shows that theoretical predictions are slightly lower than the experimental classical-flutter speeds, but are possibly adequate for predicting classical flutter; however, the theoretical values are considerably higher than the experimental stall-flutter speeds, which indicate that classical theory, using oscillating air forces derived from potential flow, is wholly inadequate for predicting stall-flutter speeds.

It would be less time consuming to compute the classical-flutter speed of a given propeller if two-dimensional wing-flutter theory, rather than the more tedious propeller-flutter theory, could be used. This could be done if a representative section on the propeller blade were established at which a flutter speed computed by two-dimensional theory could be applied. Calculations by the wing-flutter theory of reference 7 were made on the three models used to compare theory and experiment, and the results are shown in column (3), table III. On the basis of comparing the two-dimensional calculations with the propeller calculations in column (2), theoretically derived representative sections are determined and are listed in column (4). These results show that a value of 75 percent blade length may be adequate for the representative section.

## CONCLUSIONS

The effect of many parameters significant to wing flutter as well as blade twist was studied on several untwisted rotating models to determine their significance with respect to propeller stall flutter. The experimental propeller-flutter data indicate the following conclusions:

1. The minimum flutter-speed coefficients obtained at low Mach numbers were slightly greater than 1.0.
2. Forward movement of the section center-of-gravity location, increasing section thickness ratio, sweepback, and Mach number at supercritical speeds were the only parameters studied that raised the minimum flutter-speed coefficients appreciably above 1.0. Section center-of-gravity location and Mach number appeared to show the most significant increases.
3. The beneficial effect of Mach number indicates a design parameter which is designated by  $(b\omega_n/c)_{0.8L}$ , where  $b$  is the semichord taken at 0.8 blade length  $L$ ,  $\omega_n$  is the natural first-torsion circular frequency of the blade, and  $c$  is the sound speed of the operating medium. It appears that a tentative design criterion can be given which states that propeller blades having  $(b\omega_n/c)_{0.8L}$  greater than 0.50 should be entirely free of flutter.
4. Practical supersonic propellers having thin blade sections may not satisfy the criterion. A proper cycling procedure would then probably be necessary whereby the propeller could be accelerated to supersonic speeds at low blade angles. For this procedure to be successful, the classical-flutter speed must be appreciably higher than the desired operating speed. Once the propeller is up to speed, the blade angle can be increased to the desired loading conditions without encountering flutter.

Langley Aeronautical Laboratory,  
National Advisory Committee for Aeronautics,  
Langley Field, Va., December 12, 1950.

## APPENDIX

## METHOD OF ANALYSIS

The classical wing-flutter theory of reference 10 was modified for application to propellers in the following manner.

The equations of equilibrium in the torsional and bending degrees of freedom are written in reference 10 with the sweepback terms neglected as

$$\left( \underline{h}A_2 + \underline{\theta}B_2 \right) \pi \rho b_r^3 \omega^2 = 0 \quad (1)$$

$$\left( \underline{h}D_2 + \underline{\theta}E_2 \right) \pi \rho b_r^4 \omega^2 = 0 \quad (2)$$

where

$$A_2 = \left[ 1 - \left( \frac{\omega h}{\omega} \right)^2 (1 + i g_h) \right] \frac{L}{b_r} \int_0^{1.0} \left( \frac{b}{b_r} \right)^{\frac{2}{\kappa}} [F_h(\eta)]^2 d\eta -$$

$$\frac{L}{b_r} \int_0^{1.0} \left( \frac{b}{b_r} \right)^2 A_{ch} [F_h(\eta)]^2 d\eta \quad (3a)$$

$$B_2 = L \int_0^{1.0} \left( \frac{b}{b_r} \right)^3 \left( \frac{x_\alpha}{\kappa} - A_{c\alpha} \right) [F_h(\eta)] [F_\theta(\eta)] d\eta \quad (3b)$$

$$D_2 = \frac{L}{b_r} \int_0^{1.0} \left( \frac{b}{b_r} \right)^3 \left( \frac{x_\alpha}{\kappa} - A_{ah} \right) [F_h(\eta)] [F_\theta(\eta)] d\eta \quad (3c)$$

$$E_2 = L \left[ 1 - \left( \frac{\omega_\alpha}{\omega} \right)^2 (1 + i g_\alpha) \right] \int_0^{1.0} \left( \frac{b}{b_r} \right)^4 \frac{r_\alpha^2}{\kappa} \left[ F_\theta(\eta) \right]^2 d\eta -$$

$$L \int_0^{1.0} \left( \frac{b}{b_r} \right)^4 A_{\alpha\alpha} \left[ F_\theta(\eta) \right]^2 d\eta \quad (3d)$$

The air forces are given by

$$A_{ch} = -1 - \frac{2G}{k} + i \frac{2F}{k}$$

$$A_{c\alpha} = a + \frac{2F}{k^2} - \left( \frac{1}{2} - a \right) \frac{2G}{k} + i \left[ \frac{1}{k} + \frac{2G}{k^2} + \left( \frac{1}{2} - a \right) \frac{2F}{k} \right]$$

$$A_{ah} = a + \left( \frac{1}{2} + a \right) \frac{2G}{k} + i \left( \frac{1}{2} + a \right) \left( - \frac{2F}{k} \right) = - \frac{1}{2} - \left( \frac{1}{2} + a \right) A_{ch}$$

$$A_{\alpha\alpha} = - \frac{1}{8} - a^2 - \left( \frac{1}{2} + a \right) \frac{2F}{k^2} + \left( \frac{1}{4} - a^2 \right) \frac{2G}{k} +$$

$$i \left[ \left( \frac{1}{2} - a \right) \frac{1}{k} - \left( \frac{1}{4} - a^2 \right) \frac{2F}{k} - \left( \frac{1}{2} + a \right) \frac{2G}{k^2} \right]$$

The quantities  $F$  and  $G$  are the real and imaginary parts, respectively, of the complex function  $C = C(k) = F(k) + iG(k)$  which is associated with the wake and was developed by Theodorsen in reference 11.

The border-line condition of flutter separating the damped and undamped oscillations is determined by a nontrivial solution of the homogeneous equations (1) and (2). The flutter condition is solved by

means of the vanishing determinant of the coefficients of the bending and torsional motions,

$$\begin{vmatrix} A_2 & B_2 \\ D_2 & E_2 \end{vmatrix} = 0 \quad (4)$$

This wing-flutter theory was applied to propellers by integrating the air forces over the blade as follows: For blades with constant chord, the velocity and hence  $1/k$  varies directly with radius; therefore, the air forces must be integrated with respect to  $\eta'$  which equals  $\frac{H+X}{H+L}$ . Since the elements of the determinant are obtained by integrating with respect to  $\eta$ , it is advisable to set down the air-force terms in such a form that they are also functions of  $\eta$  instead of  $\eta'$ :

$$\eta' = \frac{H+X}{H+L} \quad (5a)$$

$$\eta = \frac{X}{L} \quad (5b)$$

Therefore,

$$\eta' = \frac{H+\eta L}{H+L} \quad (5c)$$

At this point it appears most convenient to set up the integrals involving the air-force terms in the form of summations for use in a solution by strip analysis.

In  $A_2$ , the term

$$\frac{L}{b_r} \int_0^{1.0} \left(\frac{b}{b_r}\right)^2 A_{ch} \left[ F_h(\eta) \right]^2 d\eta$$

becomes

$$\frac{L}{b_r} \sum_0^{1.0} \left(\frac{b}{b_r}\right)^2 [F_h(\eta)]^2 \left(-1 - \frac{2G}{k} + i \frac{2F}{k}\right) \Delta\eta \quad (6)$$

By taking the reference section at the tip,  $1/k$  at any point along the blade is equal to  $\frac{1}{k_{tip}} \eta' \frac{b_r}{b}$  which would correspond to the resultant velocity for the condition of zero forward velocity. In forward flight the resultant velocity along the blade would not vary linearly with radius, and would be a function also of the forward velocity. For zero forward velocity,  $1/k$  according to equation (5c) becomes

$$\frac{1}{k_{tip}} \frac{H + i\eta L}{H + L} \frac{b_r}{b} \quad (7)$$

Equation (6) can then be written as follows:

$$\frac{L}{b_r} \sum_0^{1.0} \left(\frac{b}{b_r}\right)^2 [F_h(\eta)]^2 \left[-1 + \left(-2G + 2iF\right) \frac{b_r}{b} \frac{H + \eta L}{H + L} \frac{1}{k_{tip}}\right] \Delta\eta$$

It should be noted that the aerodynamic coefficients  $F$  and  $G$  are related to the local values of  $1/k$  and thus vary along the blade radius also. For the purpose of strip analysis,  $\eta$  must be measured to the center of each strip.

Continuing the same procedure for each of the four determinant elements, equations (3), results in the following equations. Only the parts containing the air-force terms are shown as summations, because the mass terms can be integrated mathematically for untapered blades.

$$A_2 = \left[1 - \left(\frac{\omega_h}{\omega}\right)^2 (1 + i g_h)\right] \frac{L}{b_r} \int_0^{1.0} \left(\frac{b}{b_r}\right)^2 \frac{1}{k} [F_h(\eta)]^2 d\eta -$$

$$\frac{L}{b_r} \sum_0^{1.0} \left(\frac{b}{b_r}\right)^2 [F_h(\eta)]^2 \left[-1 + \left(-2G + 2iF\right) \frac{b_r}{b} \frac{H + \eta L}{H + L} \frac{1}{k_{tip}}\right] \Delta\eta \quad (8a)$$

$$B_2 = L \int_0^{1.0} \left(\frac{b}{b_r}\right)^3 \frac{x_\alpha}{\kappa} [F_h(\eta)] [F_\theta(\eta)] d\eta -$$

$$L \sum_0^{1.0} \left(\frac{b}{b_r}\right)^3 [F_h(\eta)] [F_\theta(\eta)] \left\{ a + (2F + 2iG) \left(\frac{b_r}{b}\right)^2 \left(\frac{H + \eta L}{H + L}\right)^2 \left(\frac{1}{k_{tip}}\right)^2 + \right.$$

$$\left. \left[ i - \left(\frac{1}{2} - a\right) 2G + \left(\frac{1}{2} - a\right) 2iF \right] \frac{b_r}{b} \frac{H + \eta L}{H + L} \frac{1}{k_{tip}} \right\} \Delta\eta \quad (8b)$$

$$D_2 = \frac{L}{b_r} \int_0^{1.0} \left(\frac{b}{b_r}\right)^3 \frac{x_\alpha}{\kappa} [F_h(\eta)] [F_\theta(\eta)] d\eta -$$

$$\frac{L}{b_r} \sum_0^{1.0} \left(\frac{b}{b_r}\right)^3 [F_h(\eta)] [F_\theta(\eta)] \left[ -\frac{1}{2} - \left(\frac{1}{2} + a\right) A_{ch} \right] \Delta\eta \quad (8c)$$

$$E_2 = L \left[ 1 - \left(\frac{\omega_\alpha}{\omega}\right)^2 (1 + i g_\alpha) \right] \int_0^{1.0} \left(\frac{b}{b_r}\right)^4 \frac{r_\alpha^2}{\kappa} [F_\theta(\eta)]^2 d\eta -$$

$$L \sum_0^{1.0} \left(\frac{b}{b_r}\right)^4 [F_\theta(\eta)]^2 \left\{ -\frac{1}{8} - a^2 + \right.$$

$$\left. \left[ -\left(\frac{1}{2} + a\right) 2F - \left(\frac{1}{2} + a\right) 2iG \right] \left(\frac{b_r}{b}\right)^2 \left(\frac{H + \eta L}{H + L}\right)^2 \left(\frac{1}{k_{tip}}\right)^2 + \right.$$

$$\left. \left[ \left(\frac{1}{4} - a^2\right) 2G + i\left(\frac{1}{2} - a\right) - \left(\frac{1}{4} - a^2\right) 2iF \right] \frac{b_r}{b} \frac{H + \eta L}{H + L} \frac{1}{k_{tip}} \right\} \Delta\eta \quad (8d)$$

Equations (8) are substituted into equation (4) and solved with the final result in the form of  $V/b\omega_\alpha$  as a function of  $\omega_n/\omega_\alpha$ . The effect of centrifugal force on the static bending frequency can be computed as shown in reference 12. Centrifugal force also affects the static torsion frequency, and, for the present case, the same relationship as that used to correct the bending frequency was used as a first approximation for the corrected torsion frequency. The corrected  $\omega_n/\omega_\alpha$  ratio can be computed and plotted on the same graph with the flutter calculation. The intersection of the two curves yields the theoretical flutter-speed coefficient for the given propeller.

The indicated theoretical flutter-speed coefficient is based on the torsional frequency corrected for centrifugal force. In order to compare theory with experiment, the theoretical flutter-speed coefficient should be raised by the ratio of the corrected torsional frequency to the static torsional frequency.

Mode shapes of uniform untapered beams are presented in reference 12. A method of obtaining mode shapes for nonuniform beams and beams with concentrated masses is presented in reference 13.

## REFERENCES

1. Sterne, L. H. G.: Spinning Tests on Fluttering Propellers. R. & M. No. 2022, British A.R.C., Aug. 1945.
2. Baker, John E., and Paulnock, Russell S.: Experimental Investigation of Flutter of a Propeller With Clark Y Section Operating at Zero Forward Velocity at Positive and Negative Blade-Angle Settings. NACA TN 1966, 1949.
3. Theodorsen, Theodore, and Regier, Arthur A.: Effect of the Lift Coefficient on Propeller Flutter. NACA WR L-161, 1945. (Formerly NACA ACR L5F30.)
4. Mendelson, Alexander: Effect of Centrifugal Force on Flutter of Uniform Cantilever Beam at Subsonic Speeds With Application to Compressor and Turbine Blades. NACA TN 1893, 1949.
5. Rosenberg, Reinhardt: Aero-Elastic Instability in Unbalanced Lifting Rotor Blades. Jour. Aero. Sci., vol. 11, no. 4, Oct. 1944, pp. 361-368.
6. Turner, M. J., and Duke, James B.: Propeller Flutter. Jour. Aero. Sci., vol. 16, no. 6, June 1949, pp. 323-336.
7. Theodorsen, Theodore, and Garrick, I. E.: Mechanism of Flutter - A Theoretical and Experimental Investigation of the Flutter Problem. NACA Rep. 685, 1940.
8. Huber, Paul W.: Use of Freon-12 As a Fluid for Aerodynamic Testing. NACA TN 1024, 1946.
9. Coleman, Robert P.: The Frequency of Torsional Vibration of a Tapered Beam. NACA TN 697, 1939.
10. Barmby, J. G., Cunningham, H. J., and Garrick, I. E.: Study of Effects of Sweep on the Flutter of Cantilever Wings. NACA Rep. 1014, 1951. (Supersedes NACA TN 2121.)
11. Theodorsen, Theodore: General Theory of Aerodynamic Instability and the Mechanism of Flutter. NACA Rep. 496, 1935.
12. Timoshenko, S.: Vibration Problems in Engineering. Second ed., D. Van Nostrand Co., Inc., 1937.
13. Houbolt, John C., and Anderson, Roger A.: Calculation of Uncoupled Modes and Frequencies in Bending or Torsion of Nonuniform Beams. NACA TN 1522, 1948.

TABLE I

## DESCRIPTION OF PROPELLER-FLUTTER MODELS

[Hub radius = 1.215 ft]

Model	NACA airfoil section	Blade material	$b_0/8L$ (ft)	L (ft)	$f_h$ (cps)	$f_a$ (cps)	CG (percent chord)	EA (percent chord)	$1/\kappa$ (*)	$\rho C_D^2$	$\delta h$	$\delta a$	GJ (lb-ft <sup>2</sup> )	Remarks
1a	16-003	Aluminum alloy	0.167	1.788	7.6	91.4	48.5	45	63	0.23	0.011	0.004	36	-----
1b	16-003	Aluminum alloy	.167	1.370	12.6	122.0	48.5	45	63	.23	.011	.004	36	-----
1c	16-003	Aluminum alloy	.167	.870	32.1	189.0	48.5	45	63	.23	.011	.004	36	-----
2	16-003	Aluminum alloy	.167	1.788	7.0	82.5	48.5	50	63	.23	.011	.004	36	17° twist, root to tip
3a	16-003	Steel	.167	1.788	7.2	90.5	48.5	47	177	.23	.004	.001	101	-----
3b	16-003	Steel	.167	1.788	7.6	95.0	48.5	46	177	.23	.004	.001	101	-----
3c	16-003	Steel	.167	1.370	12.8	124.5	48.5	46	177	.23	.004	.001	101	-----
3d	16-003	Steel	.167	.870	31.7	202.3	48.5	46	177	.23	.004	.001	101	-----
4	16-006	Maple	.167	1.788	13.4	81.2	48.5	47	28	.23	.02	.03	12	-----
5	16-006	Aluminum alloy	.250	1.788	20.6	176.0	48.5	44	127	.23	.011	.004	1400	-----
6	**16-003	Aluminum alloy	.199	1.750	43.7	280.5	48.5	46	76	.23	.011	.004	-----	Taper ratio = 0.57
7	16-006	Maple with brass insert at leading edge	.167	1.788	11.3	63.5	37.5	42	46	.32	.02	.03	18	-----
8	16-006	Maple with brass insert at leading edge	.167	1.788	10.5	56.2	34.0	40	56	.36	.02	.03	20	-----
9	16-006	Maple	.167	1.788	13.5	73.0	48.5	65	28	.23	.02	.03	12	Swept back 10°
10	16-006	Maple	.167	1.788	13.7	78.6	48.5	65	28	.23	.02	.03	12	Swept back 20°
11	16-006	Maple	.167	1.788	13.9	96.9	48.5	62	28	.23	.02	.03	12	Curved sweep- back, 10° at tip
12	16-006	Maple	.200	1.788	30.0	130.3	48.5	50	28	.23	.02	.03	-----	Taper ratio = 0.50
13	16-009	Maple	.167	1.788	19.0	113.0	48.5	44	42	.23	.02	.03	40	-----

\* $1/\kappa$  computed at  $\rho = 0.00238$  slug per cubic foot.\*\*Tapered in thickness,  $t/2b$  at root = 0.06 and  $t/2b$  at  $0.9L = 0.03$ .

TABLE II  
SCOPE OF PROPELLER-FLUTTER INVESTIGATIONS

Parameters studied	Range of values	Models used for studies	Figures in which parameters are evaluated
Torsional stiffness	12 to 101 lb-ft <sup>2</sup>	1a,3a,3b,4	4
Taper ratio	0.50 to 1.0	4,5,6,12	5
Blade twist (at tip)	0° and 17°	1a,2	6
Length-chord ratio	2.6 to 5.4	1a,1b,1c,3a,3b,3c,3d	7
Density of operating medium	0.0006 to 0.0024 slug/cu ft	1a	8
Section thickness ratio	3 to 9 percent chord	1a,3a,3b,4,13	9
Sweepback	0° to 20°	4,9,10,11	10
Section center-of-gravity location	34.0 to 48.5 percent chord	4,7,8	11
Mach number	0 to 1.3	5,6	12 and 13
Blade angle at 0.8L	5° to 35°	All	3 to 13

TABLE III  
COMPARISON OF CLASSICAL-FLUTTER THEORY WITH EXPERIMENTAL DATA

Model	(1)	(2)	(3)	(4)	(5) (6)	
	Theory of reference 5 ( $v/b\omega_{\alpha}$ )tip	Modified theory of reference 10 (appendix) ( $v/b\omega_{\alpha}$ )tip	Two-dimensional wing theory of reference 7, $v/b\omega_{\alpha}$	Theoretical representative section (percent blade length)	Classical flutter ( $v/b\omega_{\alpha}$ )tip	Stall flutter ( $v/b\omega_{\alpha}$ )tip
2	----	4.46	3.70	75	5.11	1.14
3a	----	7.16	6.01	76.5	----	1.24
4	3.34	3.25	2.68	75	3.41	1.14

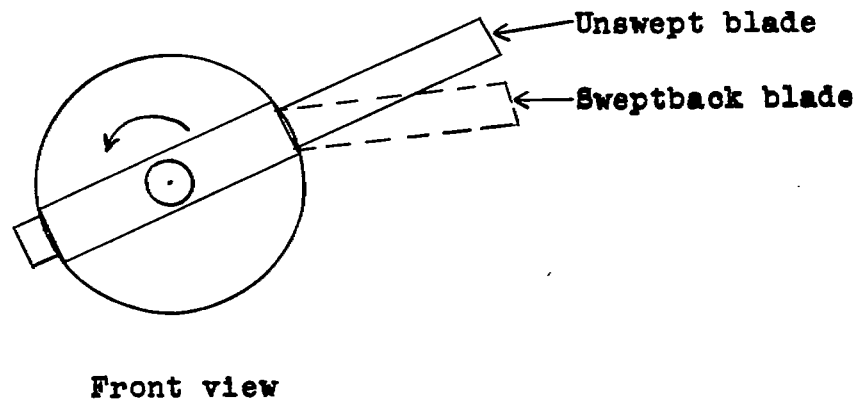
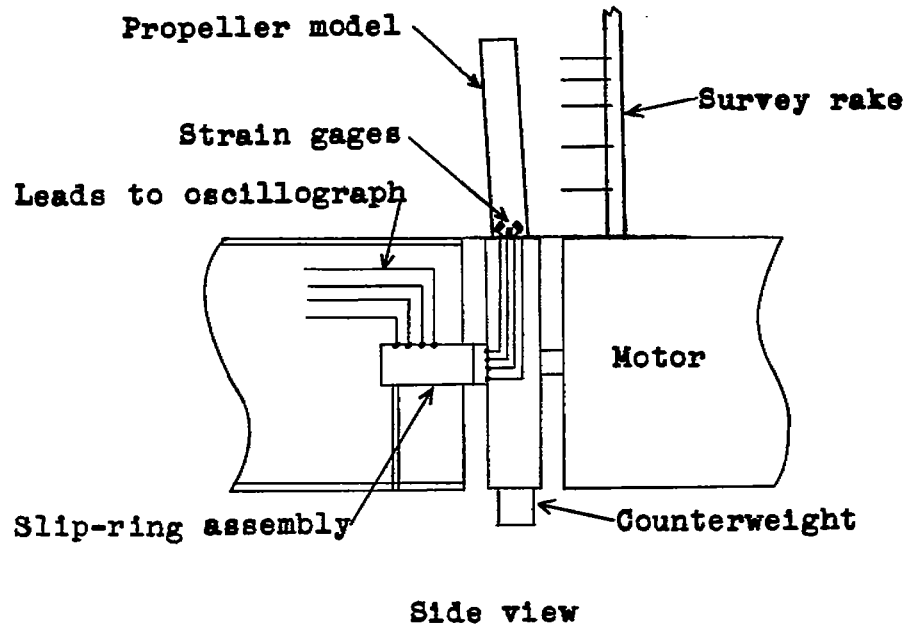


Figure 1.- Schematic diagram of propeller assembly.

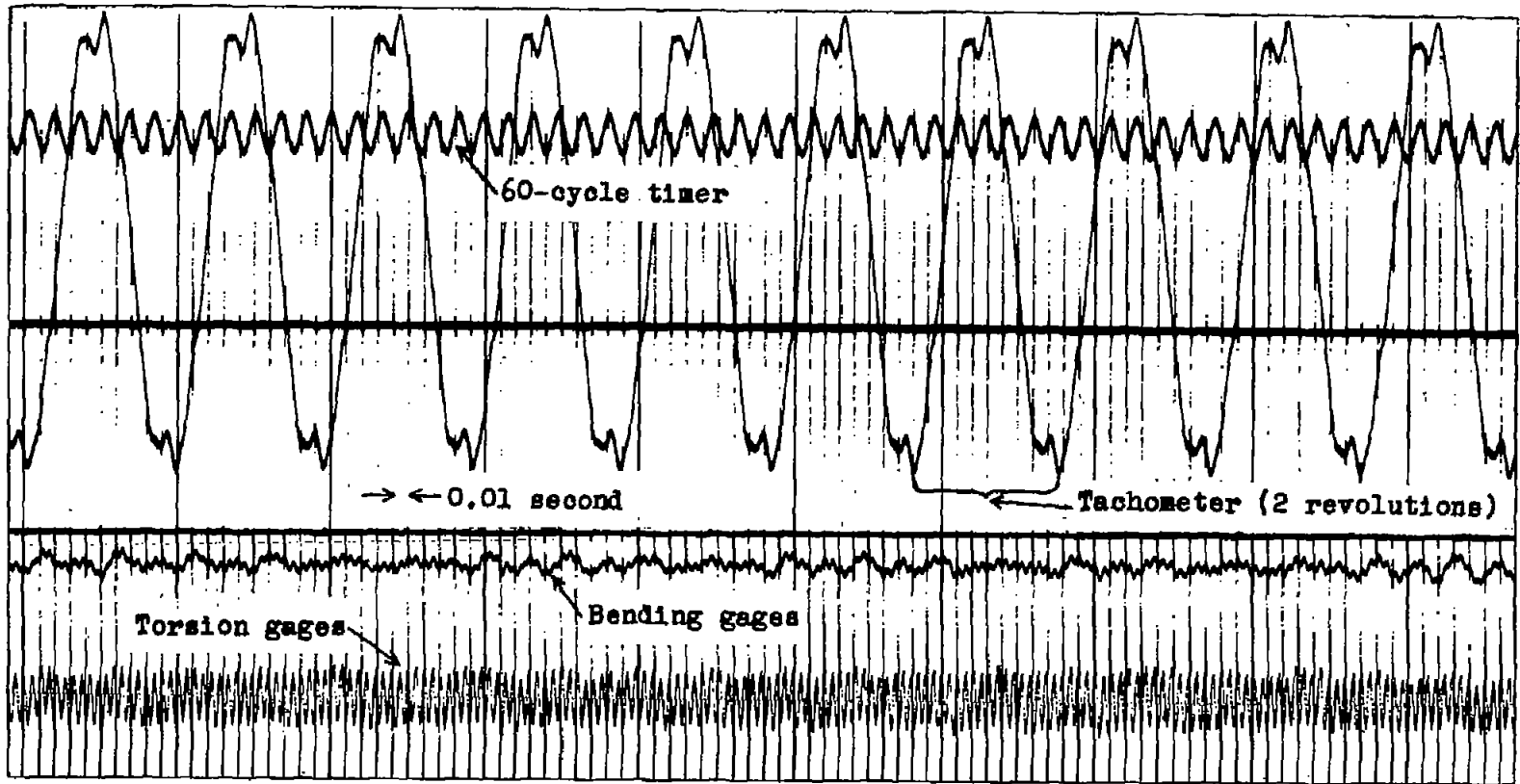


Figure 2.- Sample flutter record.

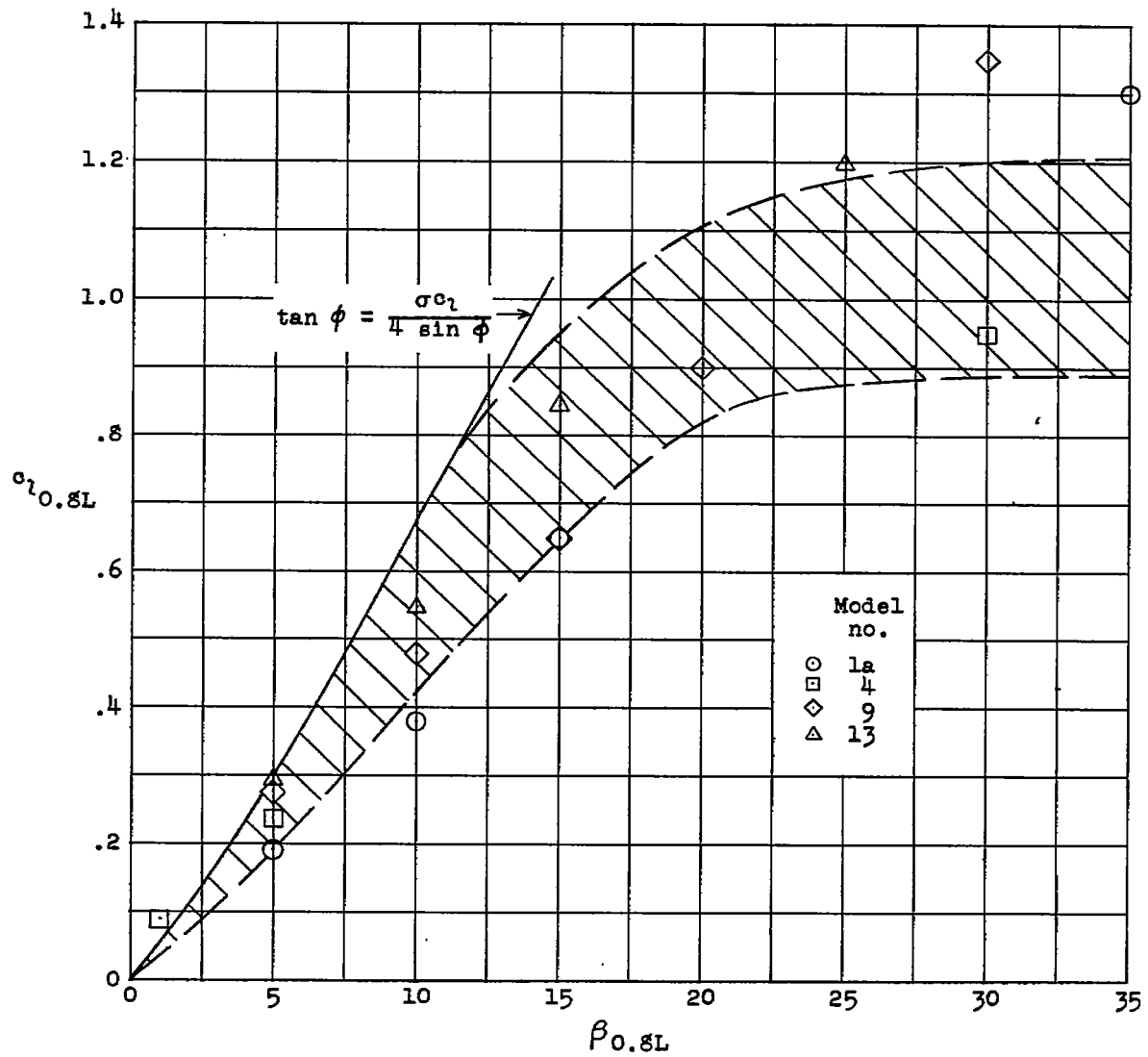


Figure 3.- Relation between lift coefficient and blade-angle setting.

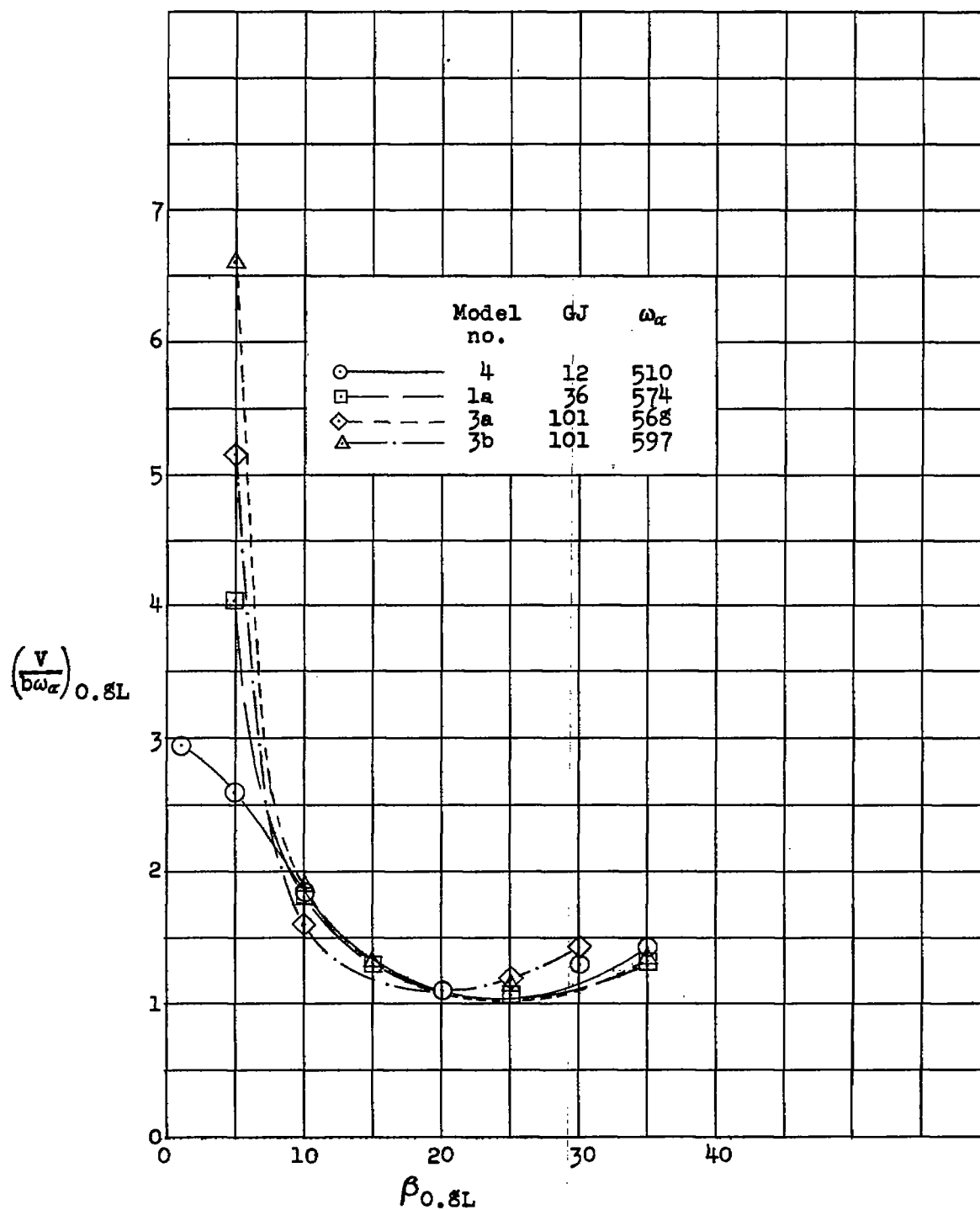


Figure 4.- Effect of torsional stiffness on flutter-speed coefficient.

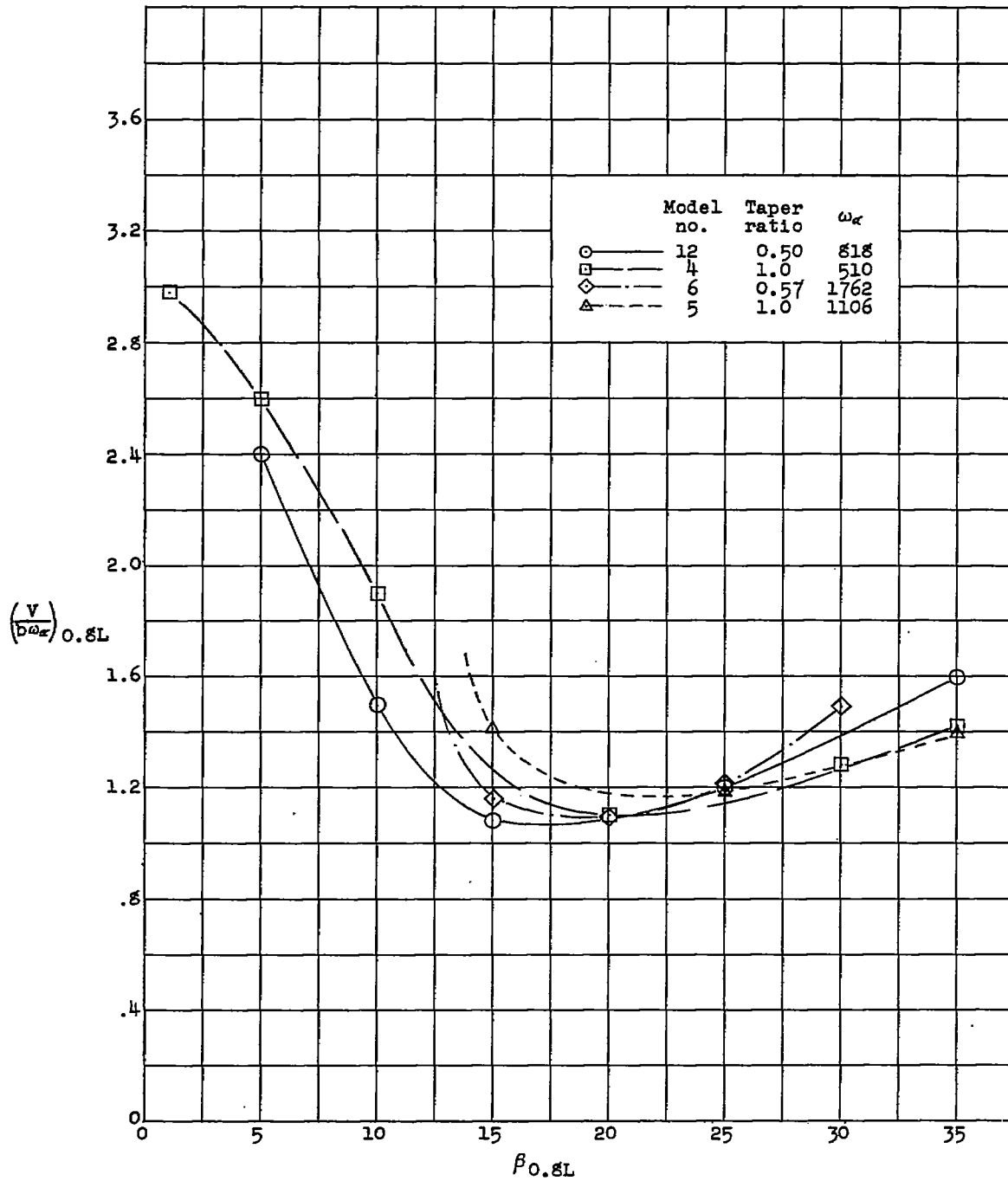


Figure 5.- Effect of blade taper on flutter-speed coefficient.

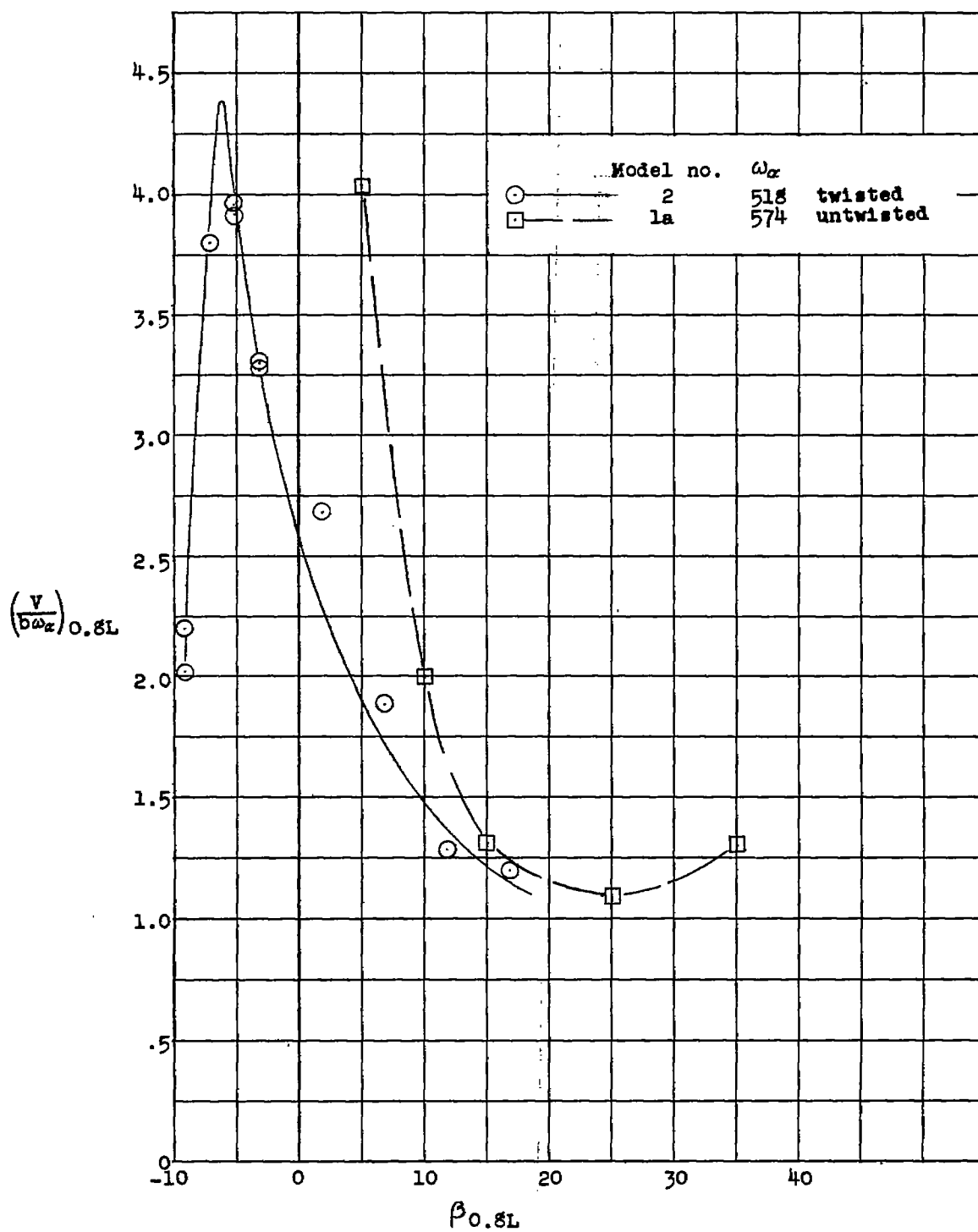
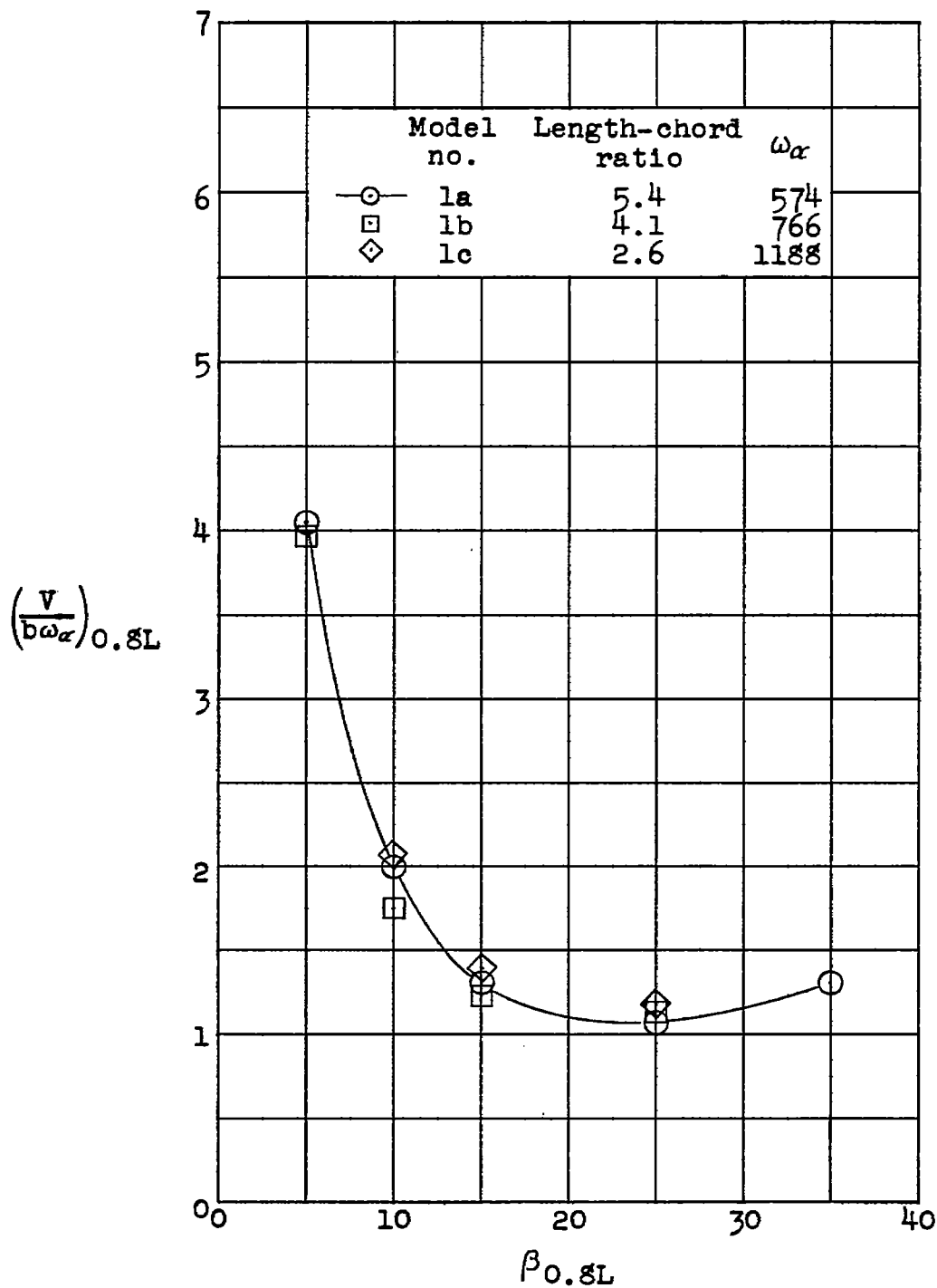
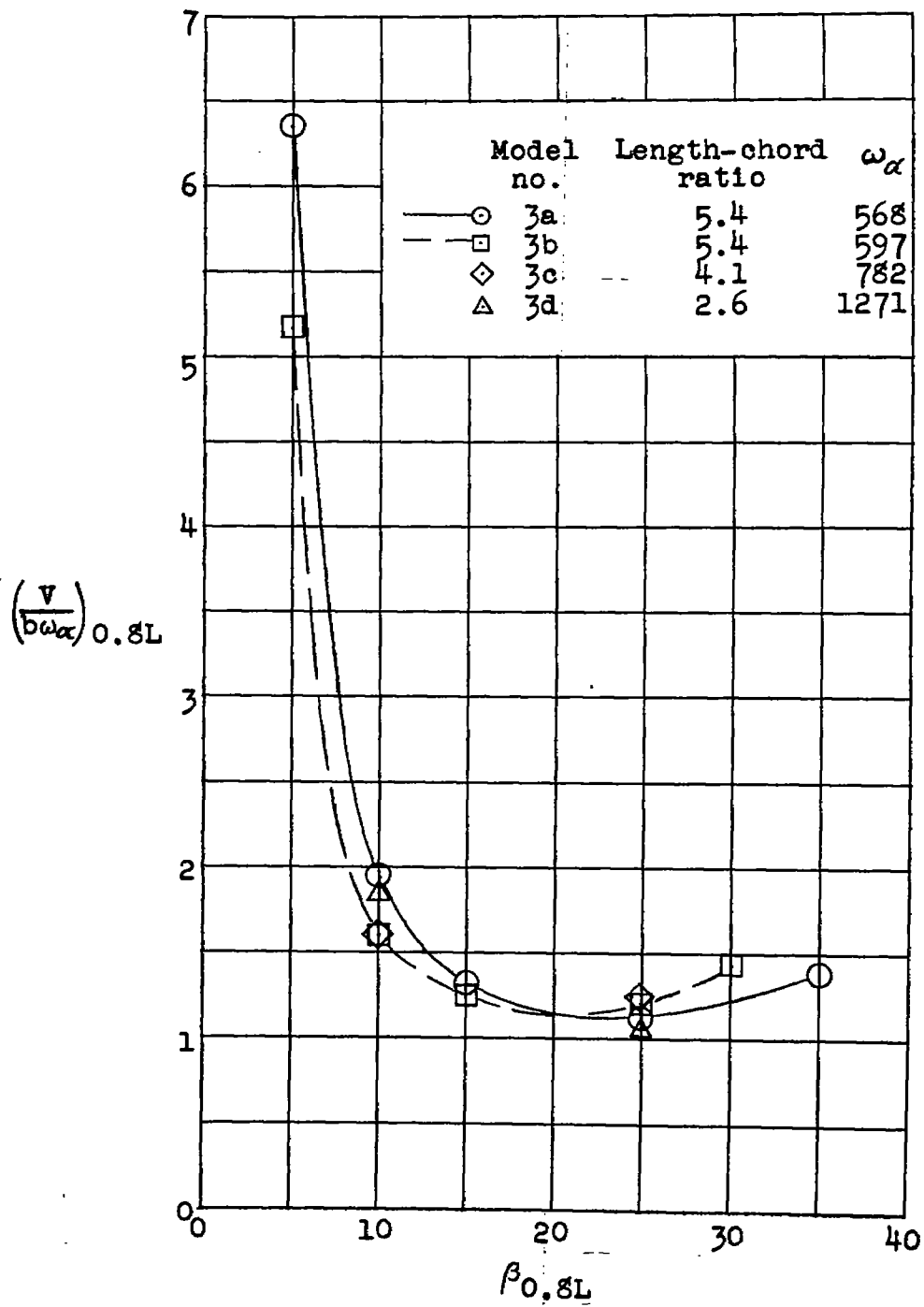


Figure 6.- Effect of blade twist on flutter-speed coefficient.



(a) Models la, lb, and lc.

Figure 7.- Effect of length-chord ratio on flutter-speed coefficient.



(b) Models 3a, 3b, 3c, and 3d.

Figure 7.- Concluded.

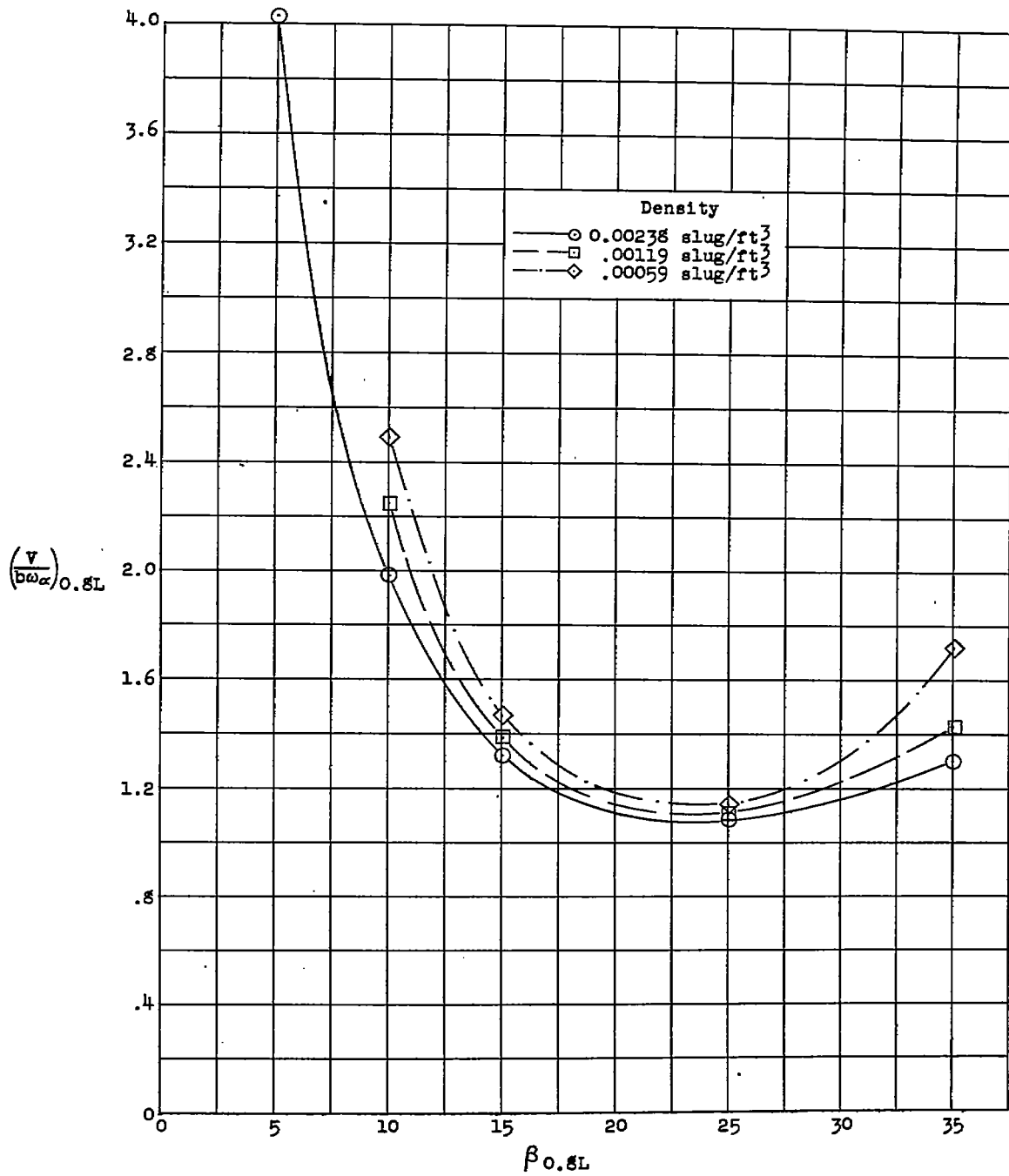


Figure 8.- Effect of density of the operating medium on flutter-speed coefficient, model 1a.

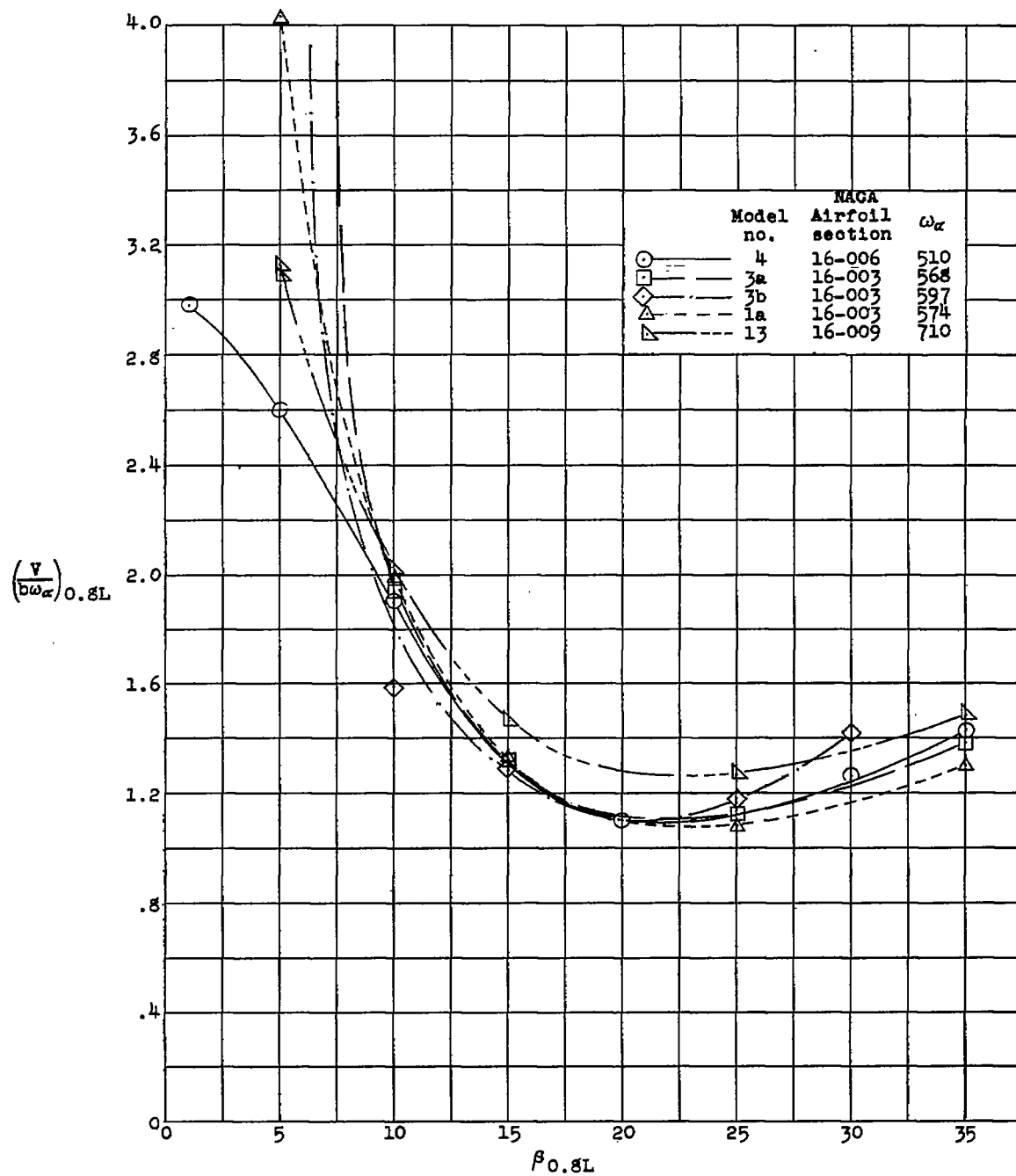


Figure 9.- Effect of section thickness ratio on flutter-speed coefficient.

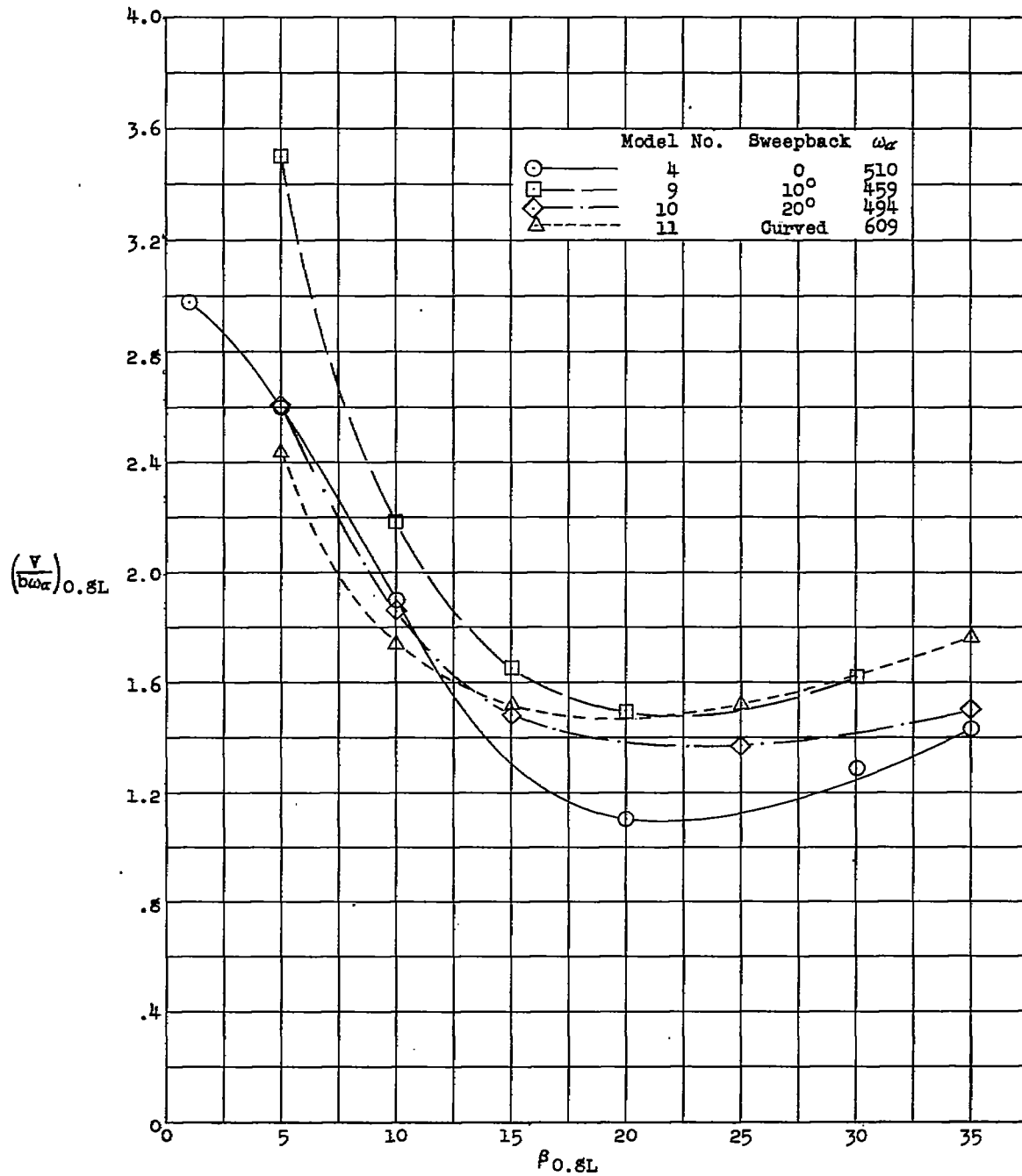


Figure 10.- Effect of sweepback on flutter-speed coefficient.

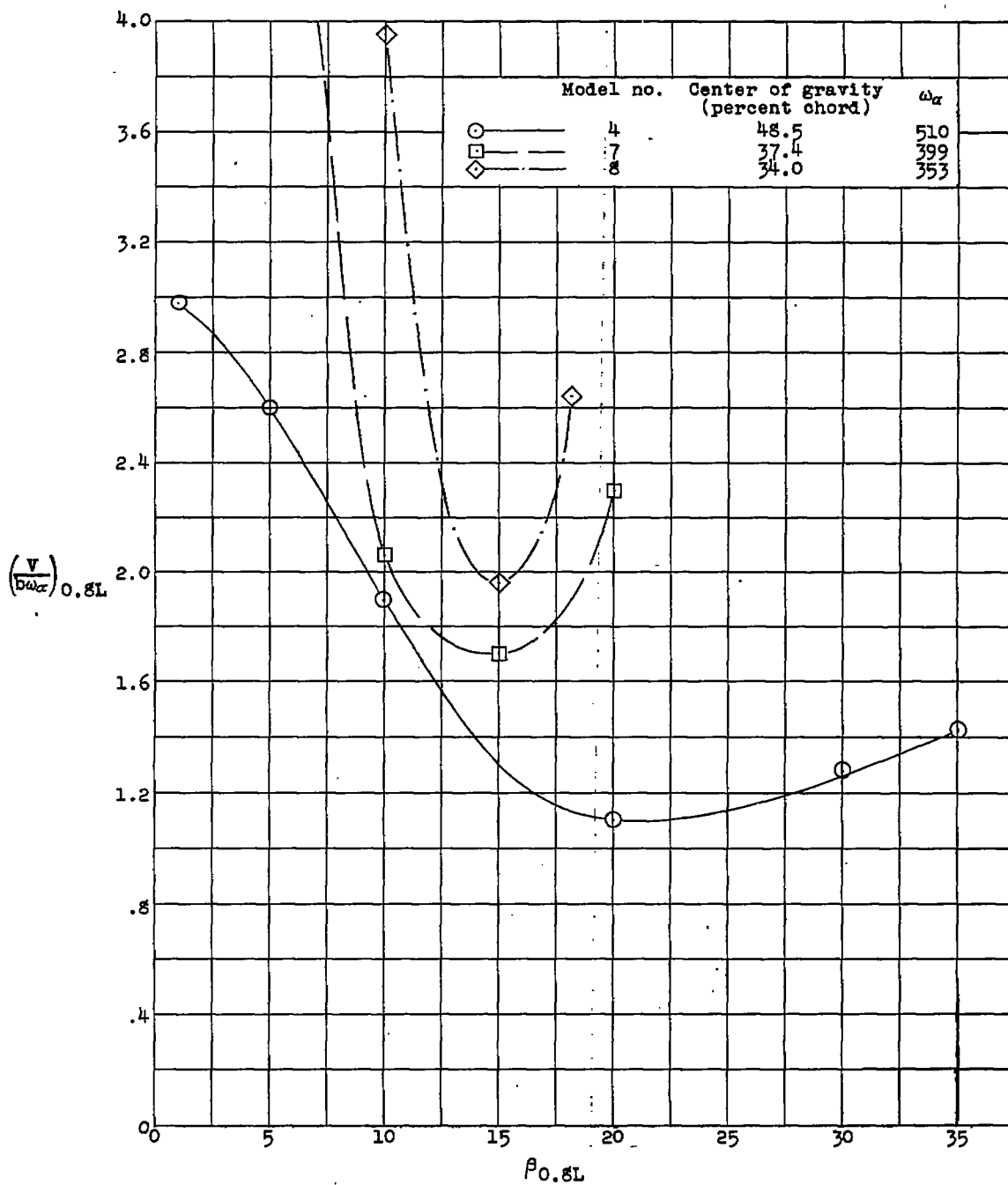
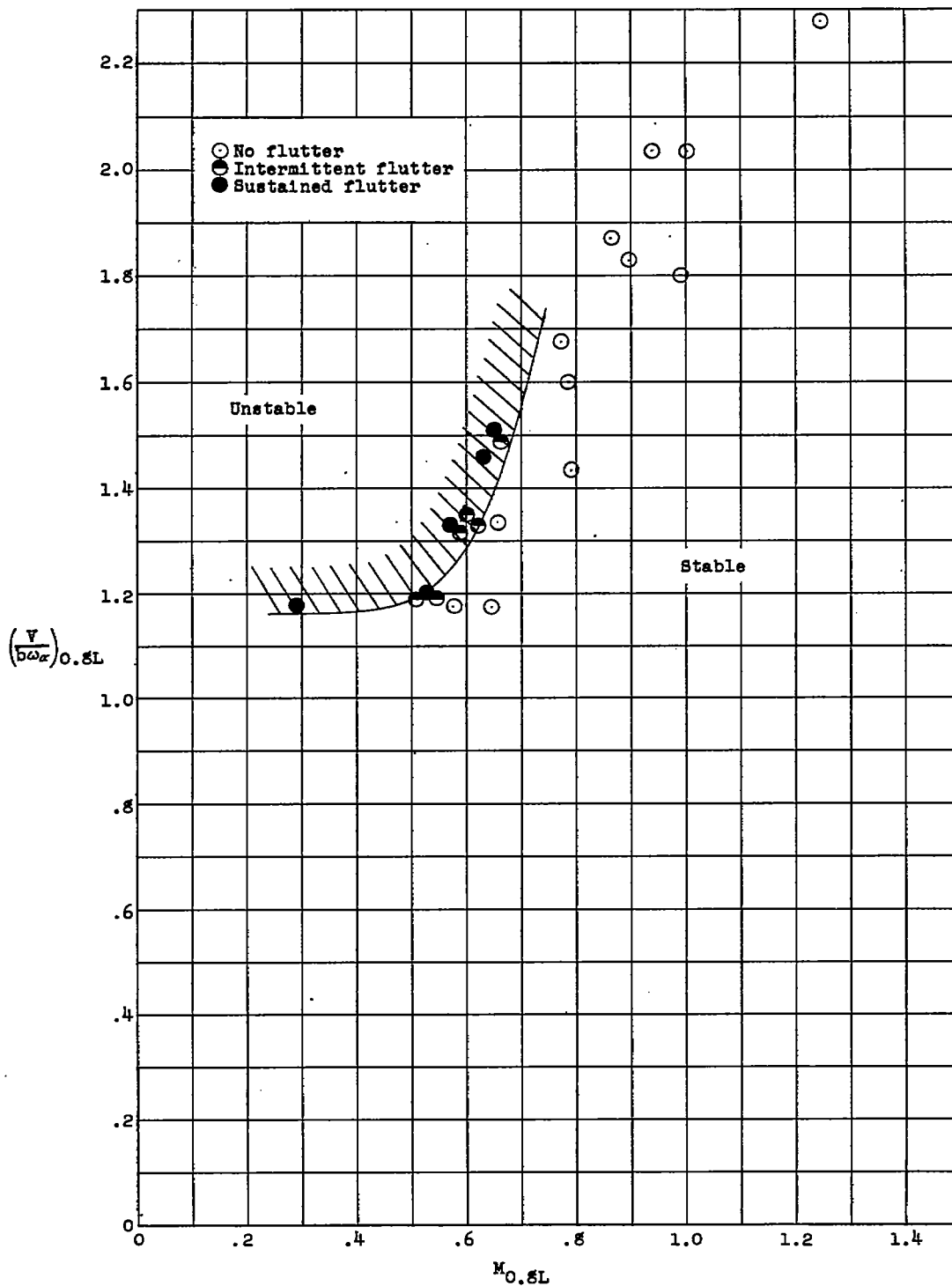


Figure 11.- Effect of section center-of-gravity location on flutter-speed coefficient.



(a) Model 5,  $\beta_{0.8L} = 25^\circ$ .

Figure 12.- Effect of Mach number on flutter-speed coefficient.

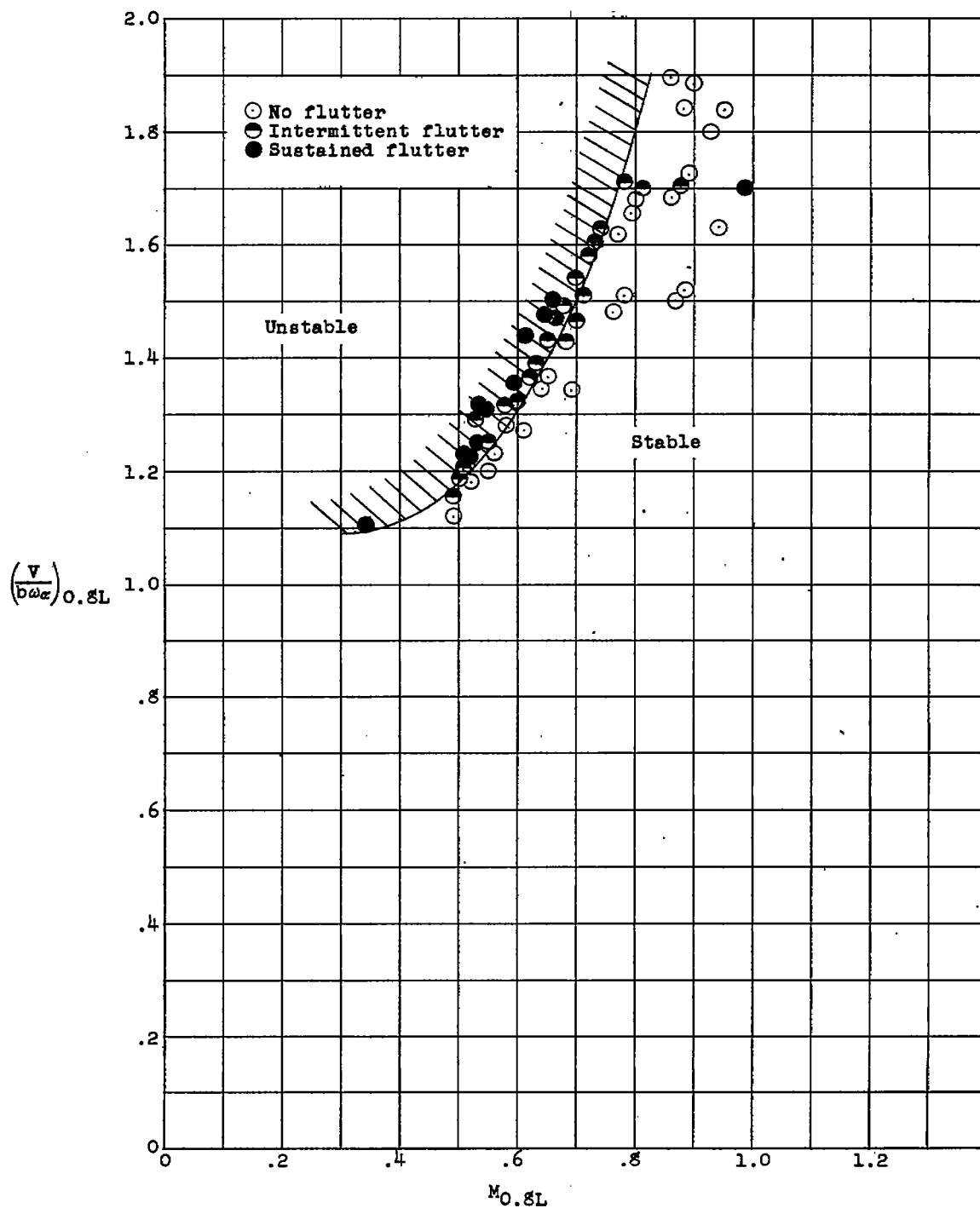
(b) Model 6,  $\beta_{0.8L} = 20^\circ$ .

Figure 12.- Concluded.

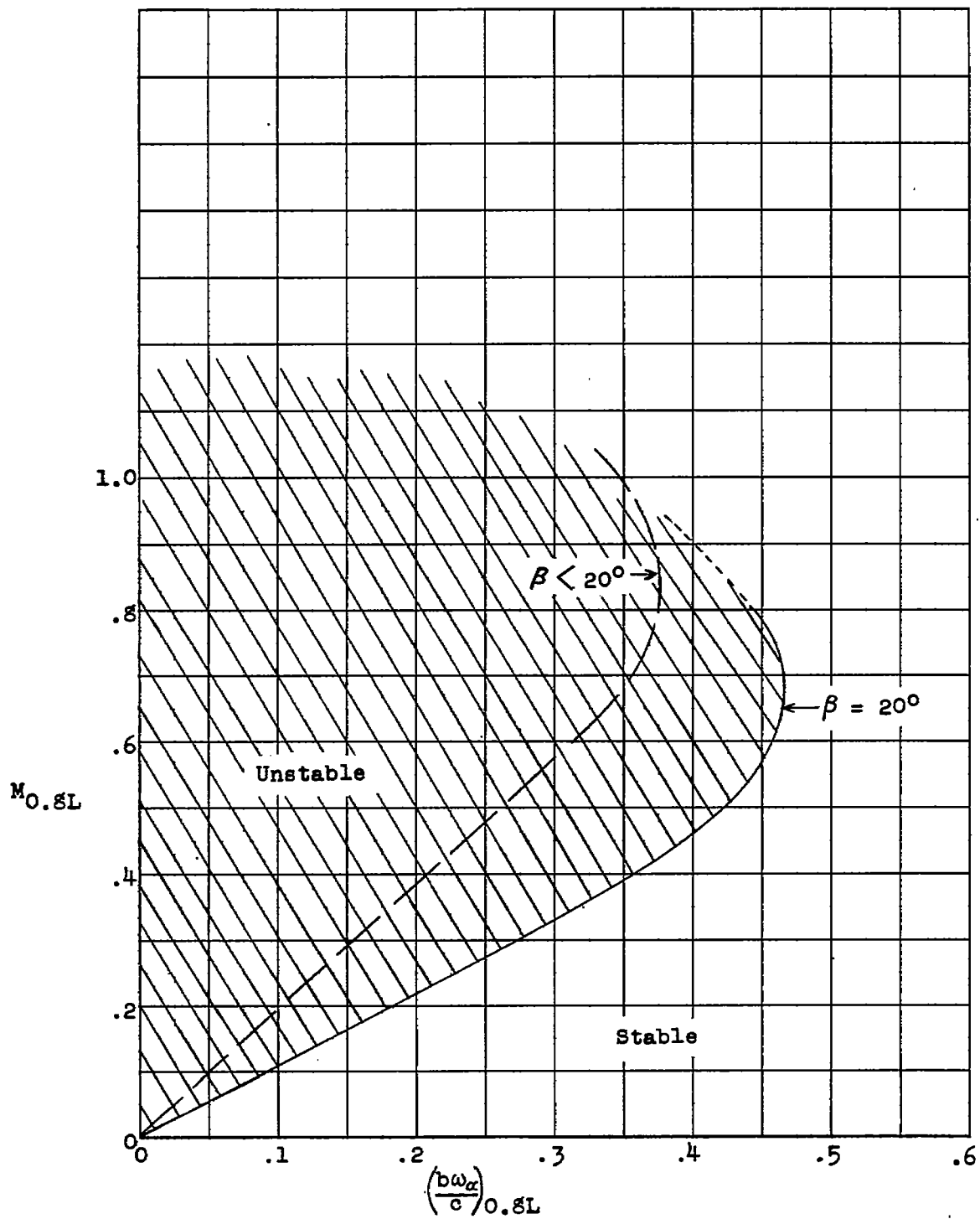


Figure 13.- Effect of Mach number on propeller flutter; model 6.

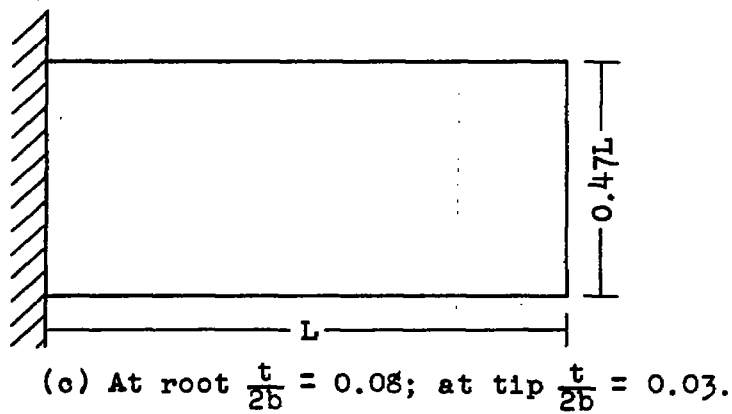
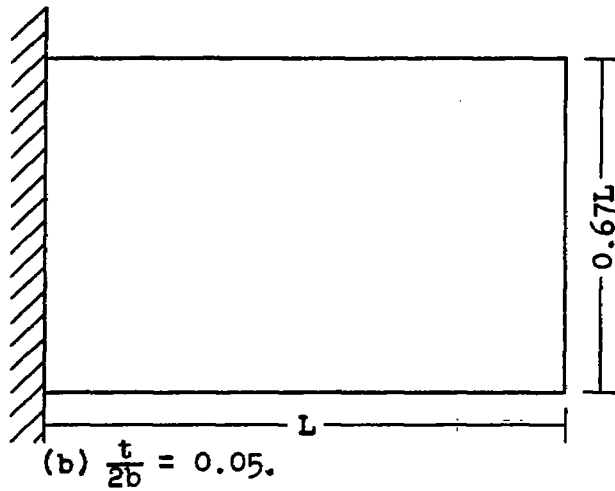
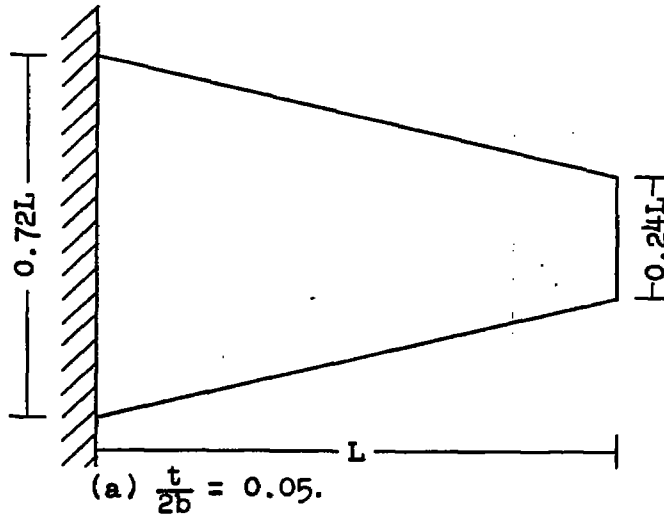


Figure 14.- Some propeller-blade configurations which satisfy the design

criterion of  $\left(\frac{bu_\alpha}{c}\right)_{0.8L} = 0.50.$  Material is aluminum alloy.